ELSEVIER

Catalysis Today 40 (1998) 85–101

CATALYSIS TODAY

Photocatalytic oxidation of organic pollutants in water

C. Domínguez[a], J. García[a], M.A. Pedraz[a], A. Torres[b], M.A. Galán[a,*]

[a]*Dpt. Ing. Química, Facultad de Ciencias Químicas, Pza Merced s/n, Universidad de Salamanca, E-37008 Salamanca, Spain*
[b]*Dpt. Ing. Química, Facultad de Ciencias, Apdo 40, Puerto Real, Cádiz, Spain*

Abstract

The primary photo-oxidation at pollutant level concentration of dodecylbenzene sulfonate (DBS), azynphos-methyl and dimethoate in water has been studied in homogeneous and heterogeneous media by using a 400 W lamp with a solar spectral distribution, and TiO_2 and $FeCl_3$ as catalysts. Two different geometries of differential batch-recycled reactors were used: first, a concentric tubular reactor with the lamp placed at the tube axis and second, a flow through parallel-plate reactor. An incidence radial model and a linear source spherical emission (LSSE) model with a Monte-Carlo approach to account for scattering of light have been used for the light intensity distribution. Data showed a molar concentration reduction of 30% for DBS in 150 min with light and TiO_2. When $FeCl_3$ was used as photocatalyst, concentration of DBS was reduced by 70%. Similar behavior found for azynphos-methyl was reduced to 85% in 20 min after irradiation with $FeCl_3$; 100% in 20 min with TiO_2 and 100% in 2 min with TiO_2 and $FeCl_3$. Approximately the same performance obtained for dimethoate was completely oxidized in 20 min after irradiation of slurry solution of TiO_2 with $FeCl_3$.

From these data kinetic equations were obtained by assuming a free-radical mechanism for oxidation of hydrocarbons. Pollutants present no activity to solar light, but when $FeCl_3$ or TiO_2 were used, pollutants were decomposed; being the value of kinetic constant of order 10^4 cm^2/einst. When the solution was irradiated with a $FeCl_3$ and TiO_2 together, the rate increased about 10 times more.

Also, deactivation of catalyst was studied by X-ray diffraction, TG and DTA methods. © 1998 Elsevier Science B.V.

Keywords: Photocatalysis; Solar light; TiO_2; Organic pollutants

1. Introduction

Growing social concern about the impact of chemicals such as pesticides, herbicides, detergents, etc. on the environment has focused attention on finding ways for more effective pollution abatement methods. Following this, one of the more promising techniques is to use a photocatalytic route to oxidize such stable chemicals [1–3].

The main objective of this work is the study of the elimination of organic pollutants in water by using solar light instead of UV light, widely used in this type of studies [4–7], and a catalyst as TiO_2. The problem is that TiO_2 absorbs light only in the narrow UV range of the solar spectrum, therefore another photocatalyst and also, probably, photosensitizer for titanium dioxide, $FeCl_3$, must be used.

Ferric ions are believed to behave as sensitizers through an electron transfer process in the ion complex $Fe^{3+}OH^-$. Ferric ion is reduced to ferrous and a hydroxyl radical OH· is formed. The latter free radical

*Corresponding author.

PII S0920-5861(97)00125-9

can initiate chain reactions, either producing some excitation of TiO_2 particles by interaction with olefinic molecules by hydrogen abstraction or by addition to them [4].

Two kind of pesticides: Azynphos-methyl ($C_{10}H_{12}NO_3PS_2$):

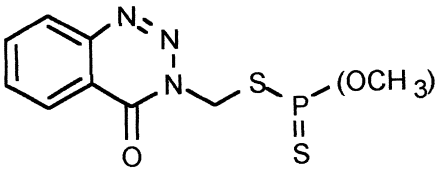

and dimethoate ($C_5H_{12}NO_3PS_2$):

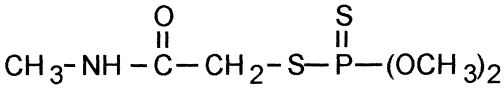

were used to study the effect of the different chain length and configuration, and also dodecylbenzene sulfonate (DBS), base of some detergents.

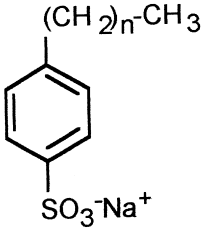

All of them have been studied at the pollutant level concentration, in the range 30–80 ppm.

2. Apparatus and experimental method

Two different reactor geometries have been used:

(i) A recycle flow-tubular reactor (details are shown in Fig. 1) with a 400 W OSRAM lamp, with a solar spectrum energy distribution (Fig. 2), placed in the axis of the reactor, the ends were blackened with black paint in order to prevent final effect of radiation and to achieve a conversion per pass through the reactor (less than 20%). Air was circulated through the annular jacket next to the lamp for cooling purposes. Distilled water or filtering solutions were circulated through the jacket in order to vary the light intensity reaching the reactor. A sleeve of aluminum blackened with several coats of black paint encompassed the reactor to prevent reflection and also to avoid outside radiation.

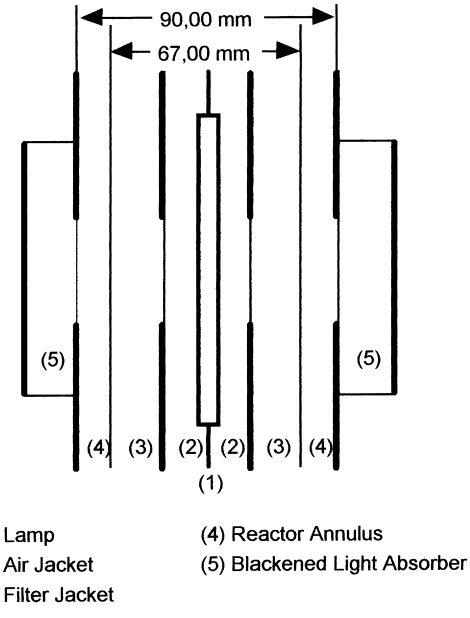

Fig. 1. Arrangement of the lamp-tubular reactor system.

Fig. 3 shows a schematic diagram of the apparatus of which the main parts are the feed tank (1), where the slurry is prepared, annular, flow-type reactor (4), and air supply system (5). To keep the oxygen concentration constant, a continuous flow of air or an air–nitrogen mixture was pumped continuously through the reservoir (1).

Some solid deposits were found on the inner wall of reactor, possibly due to $Fe(OH)_3$. To avoid this problem, another reactor geometry was used, without any physical interface between the lamp and the aqueous solution.

(ii) The reactor used was a differential parallel-plate flow reactor where the upper plate has been removed and a thin film of water is passed through the reactor. The same lamp used for the tubular reactor was placed in the focus of a specular parabolic aluminum reflector placed above the reactor, which worked as a differential recycling reactor, conversion per pass was about 6%. Details of equipment are given in Fig. 4.

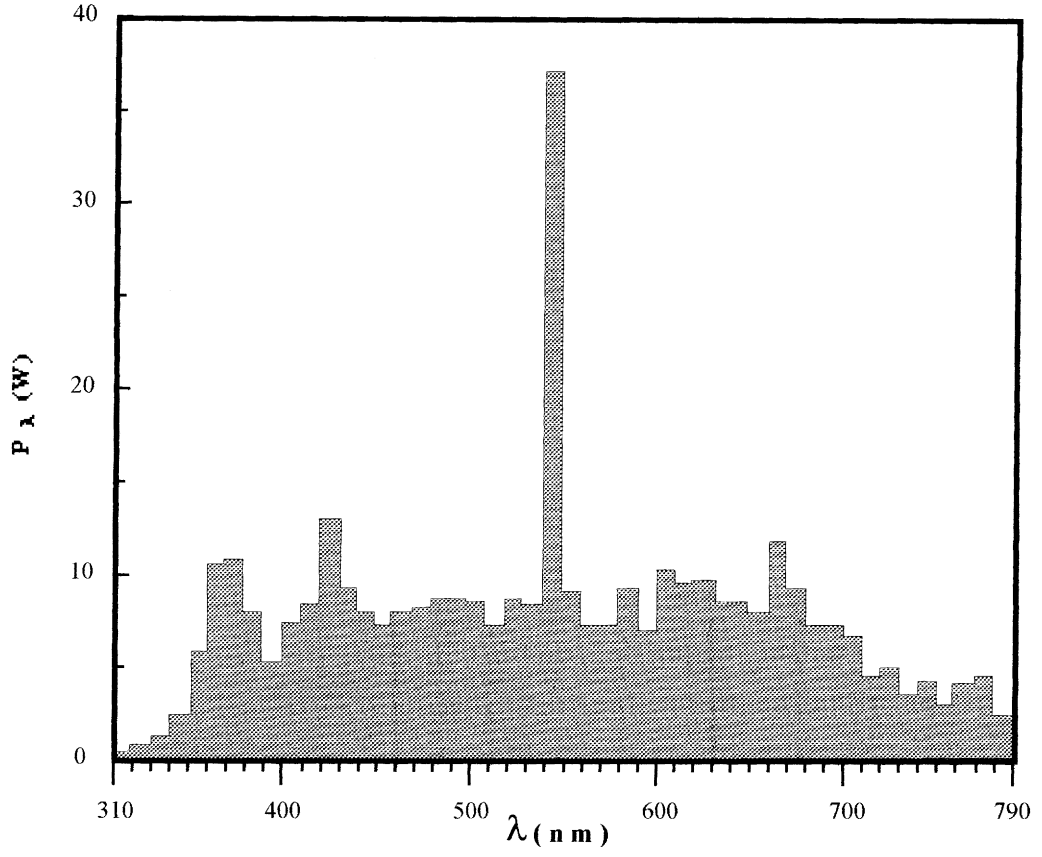

Fig. 2. Energy distribution of lamp.

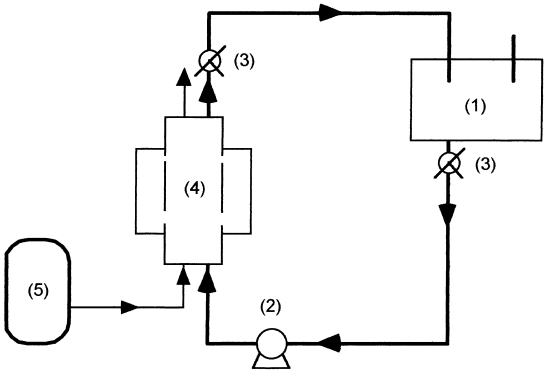

Fig. 3. Diagram of apparatus (tubular reactor).

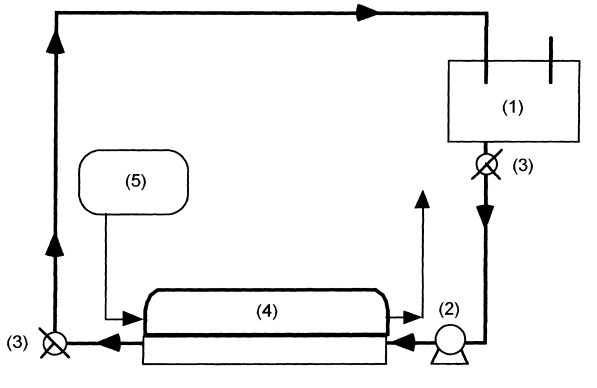

Fig. 4. Diagram of apparatus (parallel-plate reactor).

3. Mechanism of photo-oxidation

To have a framework to study this kinetics, a free-radical chain mechanism has been proposed. Briefly, this mechanism is a two-step process:

- Production of free radicals by photoactivation.
- Oxidation and reaction of free radicals to produce hydroperoxides.

The elementary steps for initial decomposition may be written:

(a) For the photo-oxidation with $FeCl_3$ through the ion complex $Fe^{3+}OH^-$.

Initiation:

$$(Fe^{3+}OH^-) \underset{\Phi\ FeCl_3}{\overset{h\nu}{\rightarrow}} (Fe^{2+}OH\cdot) \tag{1}$$

$$(Fe^{2+}OH\cdot) + P \underset{k_2}{\overset{k_1}{\rightleftarrows}} P^* + (Fe^{3+}OH^-) \tag{2}$$

Propagation:

$$P^* \overset{k_3}{\rightarrow} P\cdot \tag{3}$$

$$P\cdot + O_2 \overset{k_4}{\rightarrow} P{-}OO\cdot \tag{4}$$

$$P{-}OO\cdot + P \overset{k_5}{\rightarrow} \text{Products} + P\cdot \tag{5}$$

Termination:

$$P\cdot + W \overset{k_6}{\rightarrow} \text{End} \tag{6}$$

$$P{-}OO\cdot + W \overset{k_7}{\rightarrow} \text{End} \tag{7}$$

where P is the pollutant, P· is the free radical, P–OO· is the peroxy radical, and W is the inert (such as solvent or wall of reactor).

By assuming pseudostationary state for radicals, the kinetic equation was obtained:

$$-\Omega_p = \Phi I_{aFe^{3+}} \frac{K_4 K_5 C_{O_2} C_p}{(K_5 C_p + K_7)(K_4 C_{O_2} + K_6)}, \tag{8}$$

where Ω_p is the rate of pollutant decomposition (gmol/cm^3 s), and Φ is the quantum yield (gmol/einst).

(b) In case of photo-oxidation with TiO_2 and $FeCl_3$, the mechanism proposed is:

Initiation:

$$(Fe^{3+}OH^-) + TiO_2 \underset{\Phi}{\overset{h\nu}{\rightarrow}} (Fe^{2+}TiO_2OH\cdot)^* \tag{9}$$

$$P + (Fe^{2+}TiO_2OH\cdot)^* \underset{k'_2}{\overset{k'_1}{\rightleftarrows}} P^* + (Fe^{3+}OH^-) + TiO_2 \tag{10}$$

Propagation:

$$P^* \overset{k'_3}{\rightarrow} P\cdot \tag{11}$$

$$P\cdot + O_2 \overset{k'_4}{\rightarrow} P{-}OO\cdot \tag{12}$$

$$P{-}OO\cdot + P \overset{k'_5}{\rightarrow} \text{Products} + P\cdot \tag{13}$$

Termination:

$$P\cdot + W \overset{k'_6}{\rightarrow} \text{End} \tag{14}$$

$$P{-}OO\cdot + W \overset{k'_7}{\rightarrow} \text{End} \tag{15}$$

From this mechanism and assuming pseudostationary state, the kinetic equation was obtained:

$$-\Omega_p = \Phi I_{aFe^{3+}TiO_2} \frac{K'_4 K'_5 C_{O_2} C_p}{(K'_5 C_p + K'_7)(K'_4 C_{O_2} + K'_6)}. \tag{16}$$

I_a was the intensity absorbed by pollutants or by pollutants with $FeCl_3$, TiO_2 or $FeCl_3$–TiO_2. To calculate I_a values, it was necessary to obtain the absorptivity (α_λ) of the solutions by using a spectrophotometer equipped with a flow cell. In order to minimize the possible errors, mainly in case of slurries, these measurements were repeated three times with good agreement.

4. Analytical method

The kinetic equations Eqs. (8) and (16) show that the photo-oxidation is a function of absorbed intensity, oxygen and pollutant concentration.

Concentration of pollutants, such as DBS, azynphos-methyl and dimethoate, was determined by HPLC with a column 5A SPHERI-C-18, 20 cm length, i.d. 25 mm and a carrier of a mixture of methanol–water 50% v:v, 1,25 cm^3/min flow-rate with a UV detector, 250 nm wavelength.

For analyzing DBS, the same column was used, but the carrier was changed to a mixture of methanol–water, 73–27% v:v, with 1 cm^3/min flow-rate and a wavelength of 225 nm for the UV detector. No intermediate molecules were found with this technique.

Oxygen was continuously monitored by an oxygen electrode. The oxygen concentration was kept constant by bubbling air in all experiments, with exception of a set of them, where oxygen concentration was changed by bubbling a mixture of air–nitrogen of different concentrations through the feed-reservoir.

5. Light intensity model

To obtain the light intensity absorbed by the slurry, a model for the light distribution in the reactor–lamp system must be developed.

Two models have been used in this work:

(i) The radial model, in which it is assumed that the beam intensity is only a function of radial position [8]. This model is the simplest one and has analytical solution. The light intensity absorbed in the tubular reactor is given by

$$I_{a\lambda} = \frac{2}{R}\frac{\eta}{1-\eta^2} I_{0\lambda}\frac{F_\lambda}{F_t} T_\lambda [1 - \exp(-\mu_{a\lambda}\Delta R)], \tag{17}$$

$$\eta = \frac{r}{R}, \tag{18}$$

and for a flow parallel-plate reactor:

$$I_{a\lambda} = \frac{1}{D} I_{0\lambda}\frac{F_\lambda}{F_t} T_\lambda [1 - \exp(-\mu_{a\lambda} D)], \tag{19}$$

where $I_{0\lambda}$ is the intensity of light reaching the inner wall of reactor or the surface of solution, measured by actinometry.

(ii) The other model was a linear source spherical emission (LSSE) model [9,10] assuming the lamp as a linear source where each one of its points emits radiation in every direction and isotropically, with a Monte-Carlo method approach for solving the radiant energy balance, taking into account the absorption and scattering in the slurry reacting mixture [11].

The energy absorbed $I_{a\lambda}$ is given by

$$I_{a\lambda} = \mu_\lambda \int_{4\pi} I_{\lambda\bar{\omega}}\, d\Omega, \tag{20}$$

where

$$I_{\lambda\bar{\omega}} = I_{0,\bar{\omega}} \exp(-m_\lambda \bar{\rho}) + \int_0^{\bar{\rho}} \frac{m_\lambda C_\lambda}{4\pi} \left[\int_{4\pi} I_{\lambda\omega'} P(\omega', \omega)\, d\Omega \right] \times \exp[-m_\lambda(\bar{\rho} - \rho)]\, d\rho, \tag{21}$$

m_λ is the optical thickness and C_λ is the albedo, which represents the fraction of energy lost due to scattering, being defined by the following equations:

$$m_\lambda = (\mu_\lambda + \sigma_\lambda) R, \tag{22}$$

and

$$C_\lambda = \frac{\sigma_\lambda}{\mu_\lambda + \sigma_\lambda}, \tag{23}$$

where $I_{\lambda\omega}$ is the intensity of light in a point inside the reactor; $I_{\lambda\omega}$ was determined by 1 cm^2 photoelectric cell; P_λ is a coefficient which indicates the probability of scattering of photons inside a solid angle Ω.

6. Actinometry

Intensity of radiation reaching the wall of reactor, $I_{0\lambda}$, was measured by a chemical actinometer, the photosensitized (with uranyl sulphate) decomposition of aqueous solutions of oxalic acid. Over a range of concentration this reaction is zero-order and the attenuation factor, μ_λ, and the quantum yield, Φ_λ, are known to be a function of wavelength Eq. (8).

For a zero-order reaction a plot of $C_{A,t}$ vs. time is expected to be linear (Fig. 5). From the slope of this line and through equation

$$-\Omega_A = \frac{V_S}{V_R}\left(\frac{dC_A}{dt}\right), \tag{24}$$

the rate of decomposition can be calculated.

This rate should be equal to

$$-\Omega_A = \sum_\lambda \Phi_\lambda I_{a\lambda}, \tag{25}$$

the intensity of light reaching the wall of reactor was calculated with Eqs. (17),(19),(20) and (21), by using both models.

I_0 calculated for a tubular reactor by using the radial model for all range of wavelengths was 2.19×10^{-8}–

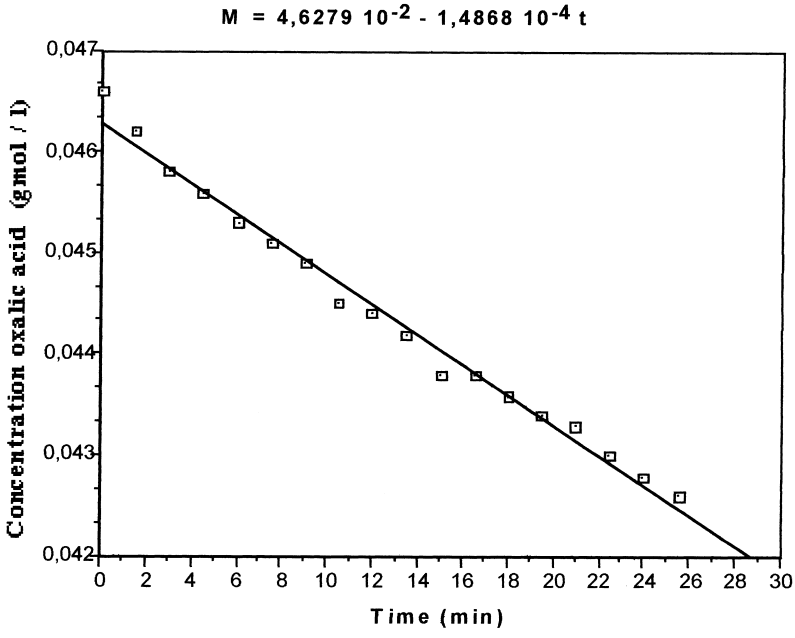

Fig. 5. Actinometer data.

2×10^{-8} eins/cm^2 s and for the LSSE model with a Monte-Carlo approach, I_0 was 2.46×10^{-8}–2.0×10^{-8} eins/cm^2 s. From these data it can be concluded that both models can be used for the light distribution, therefore the radial model was performed mainly due to its simplicity.

Actinometric runs were made at the beginning and at the end of each experiment.

7. Experimental results

7.1. Photodecomposition of DBS

Several blank runs have been made to obtain the decomposition of DBS with a concentration of 0.9×10^{-7} gmol/cm^3, in the darkness and with light but without photosensitizer (Fig. 6). No effect was found in both cases.

After that preliminary experiment in a flow-tubular reactor the decomposition of DBS when $FeCl_3$ was used as photosensitizer was verified. Then the initial rate of decomposition was measured as a function of intensity, concentration of photosensitizer and concentrations of DBS and oxygen.

The intensity absorbed was changed (modifying the $I_{0,\lambda}$) by using a filter solution of $FeCl_3$ in the range 0.013–0.025 g/l and measuring the transmittances T_λ of those solutions, and by using the radial model distribution.

A differential-flow reactor was used for these experiments with conversion per pass 5–7%, concentration of DBS was supposed to be constant, and the rate of reaction was calculated according to equation:

$$-\bar{\Omega}_{DBS} = \frac{Q}{V_R}(C_{DBS_0} - C_{DBS_L}), \tag{26}$$

where C_{DBS_0} and C_{DBS_L} were the concentrations at the entrance and exit of the reactor.

These data (Fig. 7) evidence a first-order dependence. Also, the effect of the photosensitizer concentration (0.617×10^{-7}–6.175×10^{-7} gmol/cm^3) on the rate of decomposition has been studied (Fig. 8). From these data it can be observed that for a concentration equal to or greater than C_{FeCl_3} (6.1×10^{-7} gmol/cm^3), no further change on $-\Omega_{DBS}$ was found. Therefore all experiments were performed at this concentration.

After that the effect of DBS concentration was studied working with a tubular-recycle reactor (batch) and plotting Ω_P/I_a vs. C_P keeping constant the oxygen

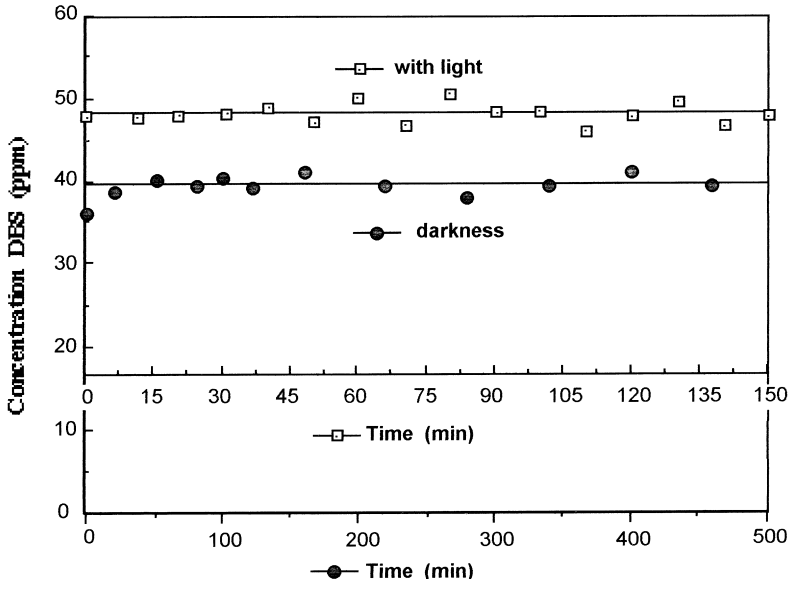

Fig. 6. Concentration of DBS (ppm) vs. time (min): (□) with solar light; (●) darkness.

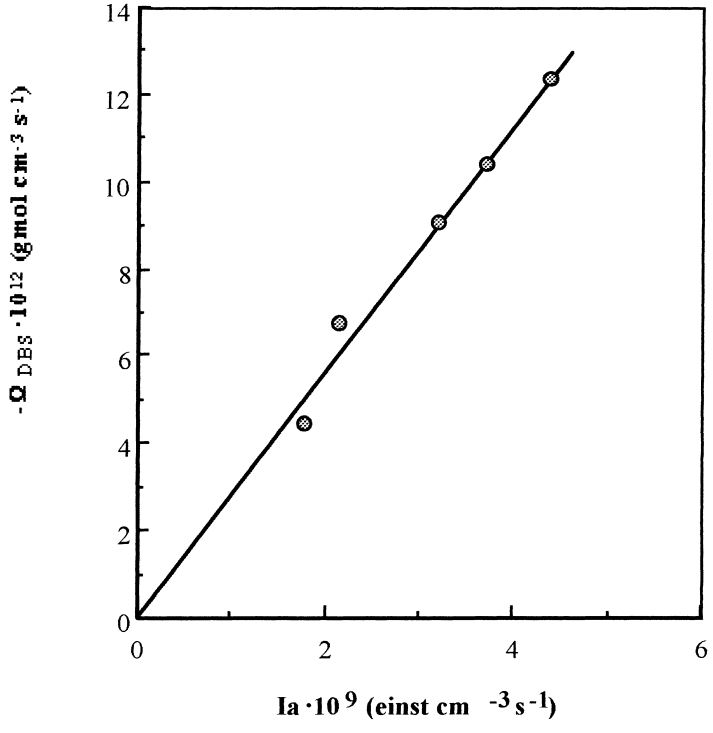

Fig. 7. Rate of decomposition of DBS·10^{12} (gmol/cm^3) vs. I_a·10^9 (einst/cm^3 s). C_{O_2}=8.9 ppm.

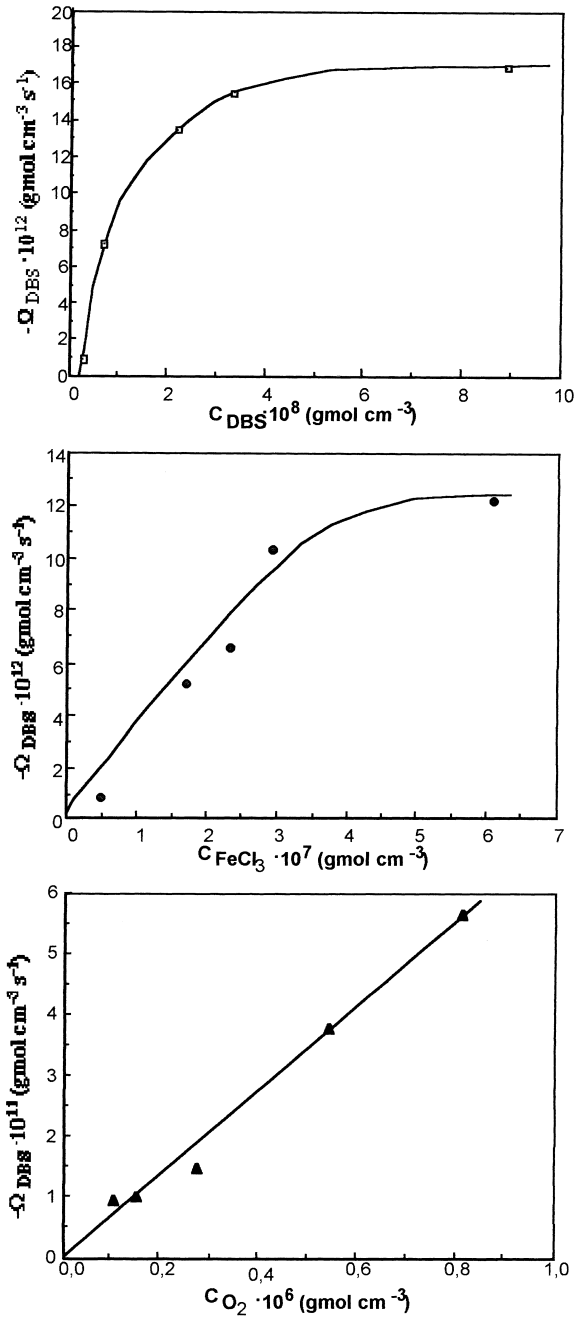

Fig. 8. (□) Rate of decomposition of DBS·10^{12} (gmol/cm^3 s) vs. $C_{DBS}\cdot10^8$ (gmol/cm^3). CO_2=8.9 ppm; C_{FeCl_3}=0.1 g/l; $I_0=1.93\times10^{-8}$ einst/cm^2 s. (●) Rate of decomposition of DBS·10^{12} (gmol/cm^3 s) vs. $C_{FeCl_3}\cdot10^7$ (gmol/l). C_{O_2}=8.9 ppm; C_{DBS}=37 ppm; $I_0=1.98\times10^{-8}$ einst/cm^2 s.(▲) Rate of decomposition of DBS·10^{11} (gmol/cm^3 s) vs. $C_{O_2}\cdot10^6$ (gmol/cm^3). C_{DBS}=15 ppm; C_{FeCl_3}=0.1 g/l; $I_0=1.98\times10^{-8}$ einst/cm^2 s.

concentration (Fig. 8). At high C_P, the rate is zero-order, while at low C_P a first-order effect is indicated according to Eq. (8).

To study the effect of oxygen concentration the liquid feed was saturated with different mixtures of nitrogen and air. The data were obtained plotted as Ω_{DBS} vs. C_{O_2} (Fig. 8) showing a linear dependence in the range of concentrations studied; therefore in Eq. (8), k_3 must be neglected vs. other terms and the product $C_{DBS}\cdot C_{O_2}$.

From all these data and by using a regression analysis method, the kinetic equation of photodecomposition of DBS photosensitized with 0.1 g/l of $FeCl_3$ was obtained:

$$-\Omega_{DBS} = 1.32\times10^{-5} I_a \left[1 + \frac{3.3\times10^{16} C_{O_2} C_{DBS}}{1 + 3.2\times10^{-7} C_{DBS}}\right]. \quad (27)$$

From this equation it can be concluded that the propagation step is faster than termination step; this dependence seems to be common for oxidation reactions.

Also these results agree with those observed by Matsuura and Smith [5], who indicate that after the initial rapid conversion of DBS molecule into a primary intermediate a slower photo-oxidation leads to small oxygenated organics.

After that, several experiments were performed adding TiO_2 powder as photocatalyst at different concentrations 2.5–0.63 gmol/l (2–0.5 g/l).

The experiments were performed with high concentration of DBS, in the range 2.3×10^{-7}–2×10^{-7} gmol/cm^3 (80–57 ppm) to have a zero-order approximation for the kinetic equation; oxygen concentration was constant (8.9 ppm) by bubbling air through the slurry reservoir, and with a concentration of 0.08 g/l of $FeCl_3$ as photosensitizer.

The data at different operation conditions were plotted as C_{DBS} vs. time and in order to compare data for different conditions, it was also plotted as $C_{DBS}-C_{DBS_0}$ vs. time (Fig. 9).

From Fig. 9 it can be concluded that for the photodecomposition of DBS with solar light, a photosensitizer must be used. Also the oxidation rate is higher for TiO_2 than with photosensitizer and the fastest reaction rate is obtained when TiO_2–$FeCl_3$ is used.

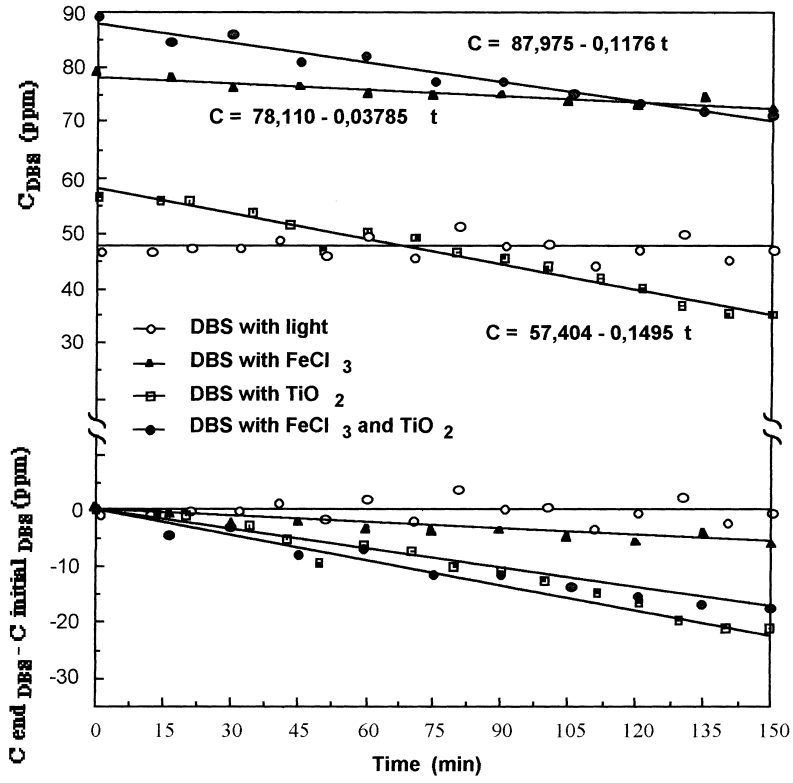

Fig. 9. Photodegradation of DBS, C_{DBS} (ppm) vs. time (min) and $Cend_{DBS}$. $Cinitial_{DBS}$ (ppm) vs. time (min). (○) DBS with light, (▲) DBS with $FeCl_3$, (□) DBS with TiO_2, (●) DBS with $FeCl_3$ and TiO_2.

Table 1
Rate of DBS oxidation (50 ppm) by using radial model and LSSE model Monte-Carlo approach at different conditions

Light distribution model	TiO_2 (g/l)	$FeCl_3$ (g/l)	$-\Omega_{DBS}$ (gmol/cm^3 s)	$-\Omega_{DBS}$ (gmol/cm^3 s g TiO_2)
Radial	2.0	0.1	2.25×10^{-11}	1.12×10^{-11}
Radial	1.0	0.1	1.11×10^{-11}	1.11×10^{-11}
LSSE Monte-Carlo	0.5	0.08	0.56×10^{-11}	1.12×10^{-11}

Table 1 presents data for rate of decomposition of DBS at concentration 50 ppm (zero-order reaction), calculated by using different concentrations of TiO_2 and $FeCl_3$ and by using both the radial model and the LSSE model with a Monte-Carlo approach taking into account the scattering of light.

From these data it can be concluded that both models lead to the same results and the effect of TiO_2–$FeCl_3$ is to increase the rate of reaction.

7.2. *Photodecomposition of azynphos-methyl*

To check the effect of TiO_2 as photocatalyst with $FeCl_3$, several studies were made by studying the oxidation of pesticides such as azynphos-methyl and dimethoate.

The azynphos-methyl in a concentration of 6.3×10^{-8} gmol/cm^3 (20 ppm) was studied in a recycle flow-tubular reactor, with the same lamp and follow-

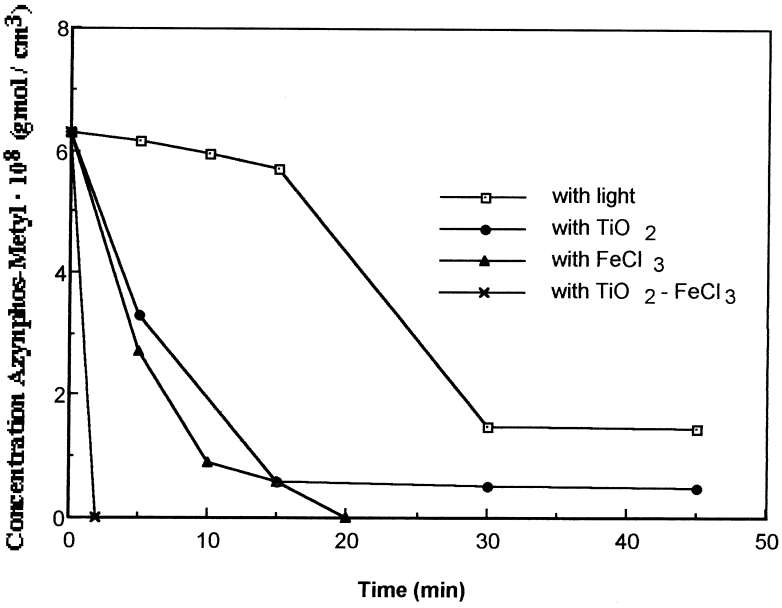

Fig. 10. Concentration of azynphos-methyl (ppm) vs. time (min): (□) with light; (●) with TiO_2; (▲) with $FeCl_3$; × with TiO_2 and $FeCl_3$.

ing the same procedure that was described before for the photo-oxidation of DBS and by using a radial model for the light distribution assuming the mechanism described in Eqs. (1)–(6) for the oxidation of hydrocarbons.

Experiments were performed to study the decomposition of this pesticide only with light, and light with concentrations of 0.1 g/l TiO_2; 0.01 g/l $FeCl_3$ and 0.1–0.01 g/l TiO_2–$FeCl_3$.

From these data (Fig. 10), it can be observed that the oxidation with TiO_2 is completed in 20 min, and with TiO_2–$FeCl_3$ in 2–3 min.

Fig. 11 shows the decomposition rate vs. azynphos-methyl concentration for different conditions. From these data the kinetics equations were obtained, with the exception to the decomposition of azynphos-methyl with light and TiO_2–$FeCl_3$, because the reaction was so fast that it was not possible to obtain enough data to determine properly the kinetic equation.

When only solar light was used the slowest steps were the initiation (radical formation):

$$A \underset{k_2}{\overset{\Phi_{P,\lambda}}{\rightleftarrows}} A^* \rightarrow A\cdot \tag{28}$$

and the kinetic equation given by regression analysis was

$$-\Omega_A = 8.5 \times 10^{-4} I_a C_A. \tag{29}$$

In case of light–TiO_2 (0.1 g/l) and light–$FeCl_3$ (0.01 g/l) the kinetic equation obtained was, for light–TiO_2:

$$\frac{-\Omega_A}{I_a} = \frac{1.06 \times 10^{-2} C_A}{0.71 \times 10^{-8} + C_A}, \tag{30}$$

and for light–$FeCl_3$:

$$\frac{-\Omega_{P_A}}{I_a} = \frac{1.36 \times 10^{-2} C_A}{1.4 \times 10^{-8} + C_A}. \tag{31}$$

From all these, it can be deduced that the decomposition rate of azynphos-methyl is almost 100 times slower than the light with $FeCl_3$ or TiO_2. However, the highest rate is obtained with a mixture of $FeCl_3$ and TiO_2.

To avoid the trouble of deposition of particles, probably of $Fe(OH)_3$ on the inner wall of reactor, another reactor geometry was used. A recycle parallel-plate flow reactor was described before as in Fig. 4. A thin film of water of 3 cm thickness was passed

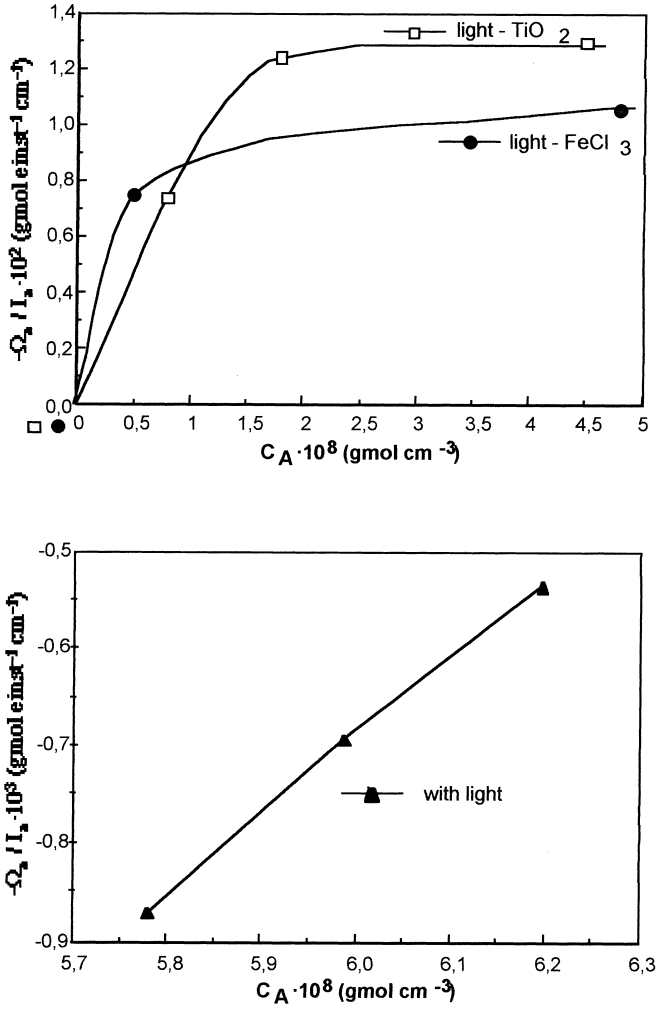

Fig. 11. (●) Rate of decomposition of azynphos-methyl/$I_a \cdot 10^2$ (gmol/einst cm) vs. $C_A \cdot 10^8$ (gmol/cm^3) with light and $FeCl_3$. (□) Rate of decomposition of azynphos-methyl/$I_a \cdot 10^2$ (gmol/einst cm) vs. $C_A \cdot 10^8$ (gmol/cm^3) with light and TiO_2. (▲) Rate of decomposition of azynphos-methyl/$I_a \cdot 10^3$ (gmol/einst cm) vs. $C_A \cdot 10^8$ (gmol/cm^3) with light.

through the reactor with a conversion per pass of about 6%. Also a plug-flow model could be assumed because no gradients of concentration were detected through the thickness of the reactor, therefore plug-flow could be assumed.

Experiments were performed at a concentration of azynphos-methyl at 30 ppm, saturation of air, oxygen concentration 2.3×10^{-7} gmol/cm^3 (8.9 ppm) and by using solar light, light with $FeCl_3$ (0.1 g/l), TiO_2 (1.0 g/l) and $FeCl_3$–TiO_2 (1.0–0.1 g/l).

Table 2
Extent of photo-oxidation of azynphos-methyl under different conditions

Conditions	Extent of degradation (%)	Time (min)
Without light	0	—
Solar light	14	100
Solar light with $FeCl_3$	62–63	180
Solar light with TiO_2	65	80
Solar light with TiO_2–$FeCl_3$	100	80

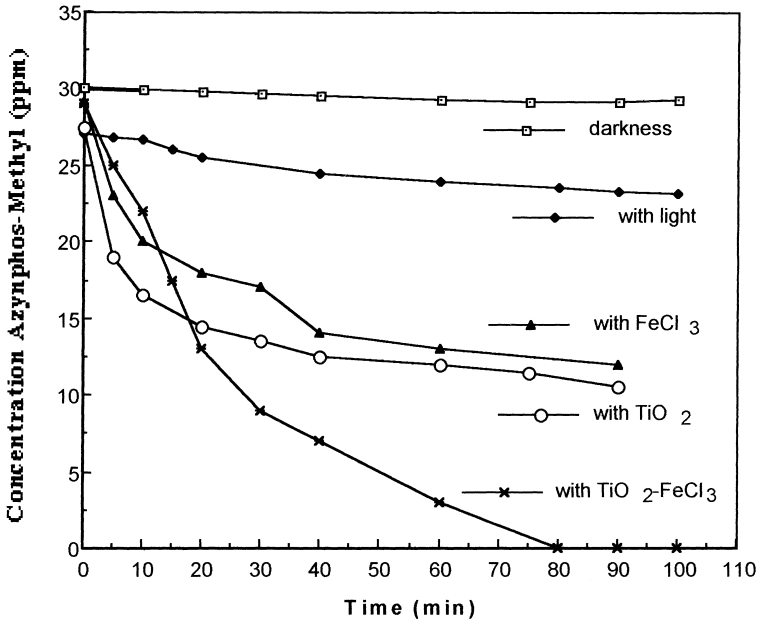

Fig. 12. Concentration of azynphos-methyl (ppm) vs. time (min): (□) darkness; (●) with light; (▲) with $FeCl_3$; (○) with TiO_2; (×) with TiO_2 and $FeCl_3$.

Data for concentration of azynphos-methyl vs. time are plotted in Fig. 12 for different conditions, and the extent of photodegradation is showed in Table 2.

For comparative purposes only data at very low concentration of azynphos-methyl were used to obtain the kinetic equation. At these conditions and from the mechanisms described before (Eq. (1)–Eq. (15)), the rate of reaction of first-order referred to absorbed intensity and azynphos-methyl concentration. Then the kinetic equation for all wavelengths and integrated over all reactor geometry is given by the following expression:

$$-\Omega_A = K^* I_a C, \tag{32}$$

where

$$K^* = K\left(\frac{1}{D}\right)\sum \Phi_\lambda \left(\frac{F_\lambda}{F_t}\right) T_\lambda \,\mathrm{cm}^2/\mathrm{einst}, \tag{33}$$

then

$$-\Omega_A = \left(\frac{1}{D}\right) K I_0 \sum \Phi_\lambda \left(\frac{F_\lambda}{F_t}\right) T_\lambda [1 - \exp \sum (\mu_\lambda C) D], \tag{34}$$

Table 3
Pseudokinetic constant for photo-oxidation of azynphos-methyl at different conditions

Conditions	K^* (cm^2/einst)
With light	4×10^{-1}
Light with 0.1 g/l $FeCl_3$	3.4×10^{4}
Light with 1 g/l TiO_2	4.6×10^{4}
Light with 0.1 g/l $FeCl_3$ and 1 g/l TiO_2	6.3×10^{5}

values of $-\Omega_A$ for a differential reactor were obtained according to Eq. (24).

Table 3 indicates K^* value for different conditions.

From these data, it can be deduced that the rate of decomposition is of the same order as before, when a tubular reactor was used: $K=10^6$ cm^2/einst.

7.3. Photodecomposition of dimethoate

Several experiments were made with other pesticide, dimethoate, because of its different chemical structure and stability. In all of them, the concentration of dimethoate was 50 ppm.

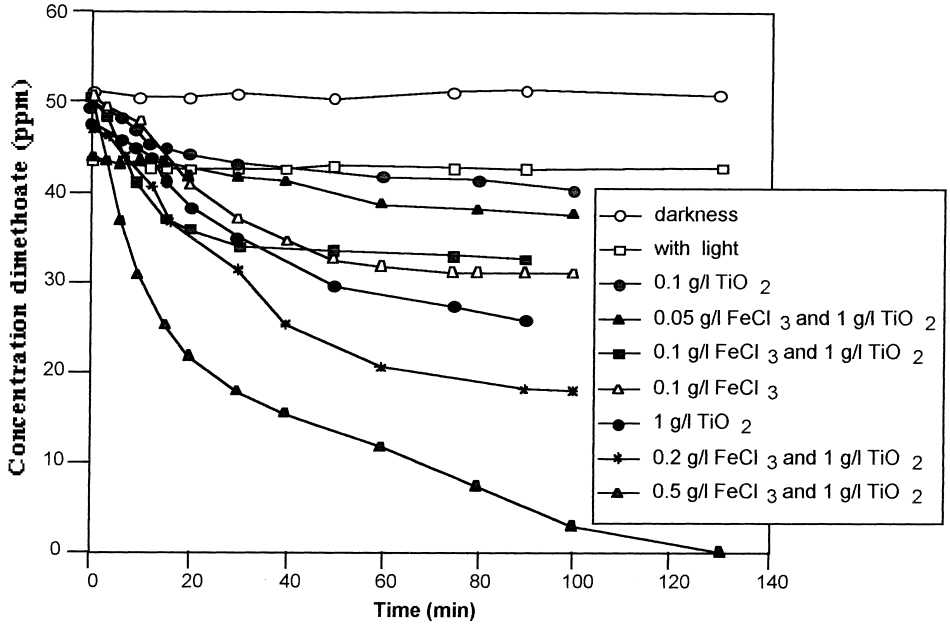

Fig. 13. Concentration of dimethoate (ppm) vs. time (min): (○) darkness; (□) with light; (●) with 0.1 g/l of TiO_2; (▲) with 0.05 g/l of $FeCl_3$ and 1 g/l of TiO_2; (■) with 0.1 g/l of $FeCl_3$ and 1 g/l of TiO_2; (△) with 0.1 g/l of $FeCl_3$; (●) with 1 g/l of TiO_2; (*) with 0.2 g/l of $FeCl_3$ and 1 g/l of TiO_2; (▲) with 0.5 g/l of $FeCl_3$ and 1 g/l of TiO_2.

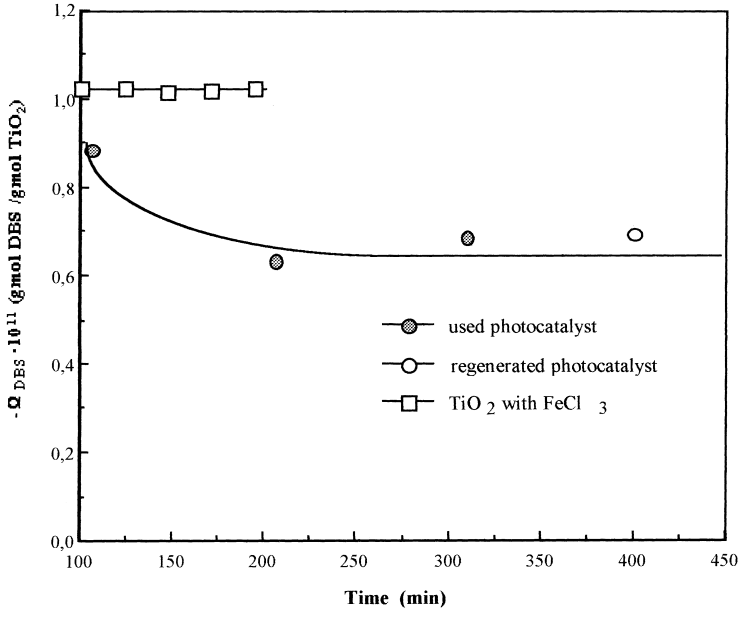

Fig. 14. Rate of decomposition of DBS·10^{11} (gmol/gmol TiO_2) vs. time (min): (●) used photocatalyst; (○) regenerated photocatalyst; (□) TiO_2 and $FeCl_3$.

Table 4
Extent of photo-oxidation of dimethoate under different conditions

Conditions	% degradated
Darkness	0
Solar light	2.1
Solar light, 0.1 g/l $FeCl_3$	38.0
Solar light, 0.1 g/l TiO_2	20.5
Solar light, 1.0 g/l TiO_2	45.4
Solar light, 0.05 g/l $FeCl_3$, 1 g/l TiO_2	21.6
Solar light, 0.1 g/l $FeCl_3$, 1 g/l TiO_2	31.2
Solar light, 0.2 g/l $FeCl_3$, 1 g/l TiO_2	65.3
Solar light, 0.5 g/l $FeCl_3$,1 g/l TiO_2	100.0

Table 5
Kinetic constants for the photo-oxidation of dimethoate under different conditions

Condition	K^* (cm^3/mol)
Solar light, 0.1 g/l $FeCl_3$	4.8×10^5
Solar light, 0.1 g/l TiO_2	3.1×10^5
Solar light, 1.0 g/l TiO_2	3.3×10^5
Solar light, 0.05 g/l $FeCl_3$, 1 g/l TiO_2	9.2×10^5
Solar light, 0.1 g/l $FeCl_3$, 1 g/l TiO_2	9.9×10^5
Solar light, 0.2 g/l $FeCl_3$, 1 g/l TiO_2	1.1×10^6
Solar light, 0.5 g/l $FeCl_3$,1 g/l TiO_2	1.3×10^6

In all these experiments, the reactor was a parallel-plate reactor mechanism and the procedure was the same as before.

The experiments were made in darkness, with light, and with light and (0.1 g/l) $FeCl_3$, (0.1–1 g/l) TiO_2 and TiO_2–$FeCl_3$ at different concentrations of $FeCl_3$ (0.05–2 g/l) and 1 g/l TiO_2.

Data are plotted in Fig. 13 and in Table 4, the percent of photodegradation of dimethoate for 100 min is shown.

From Table 4, it can be deduced that solar light oxidizes in very small extent the dimethoate. The extent of decomposition of this pesticide is larger for 0.1 g/l $FeCl_3$ than for 0.1 g/l TiO_2.

For 0.05 g/l $FeCl_3$ and 1 g/l TiO_2, the decomposition is almost the same as for 0.1 g/l TiO_2. When the amount of $FeCl_3$ is increased, keeping constant the amount of TiO_2, 1 g/l, the percent of decomposition is increased until that for 0.5 g/l $FeCl_3$ and 1 g/l TiO_2, the photodegradation is totally accomplished.

A possible explanation is: the TiO_2 activated by UV light (very narrow band in solar spectrum) is able to decompose only about 20% of dimethoate. On the other hand, 0.1 g/l of $FeCl_3$ decomposed to about 40%, and 0.1 g/l of $FeCl_3$ with 1 g/l of TiO_2 decomposed to about 30% of dimethoate. This extent is increased when the concentration of $FeCl_3$ in solution is increased for the same amount of TiO_2. That can suggest a possible intermediate between Fe^{3+} and TiO_2 or some activation of Fe^{3+} on the TiO_2.

These data were correlated according to Eqs. (33) and (34).

Kinetic constants are shown in Table 5.

From Table 5, it can be observed that the rate of photodecomposition increases when the amount of Fe^{3+} is increased for a constant concentration of TiO_2 until a value of C_{FeCl_3} is equal to 0.05 g/l.

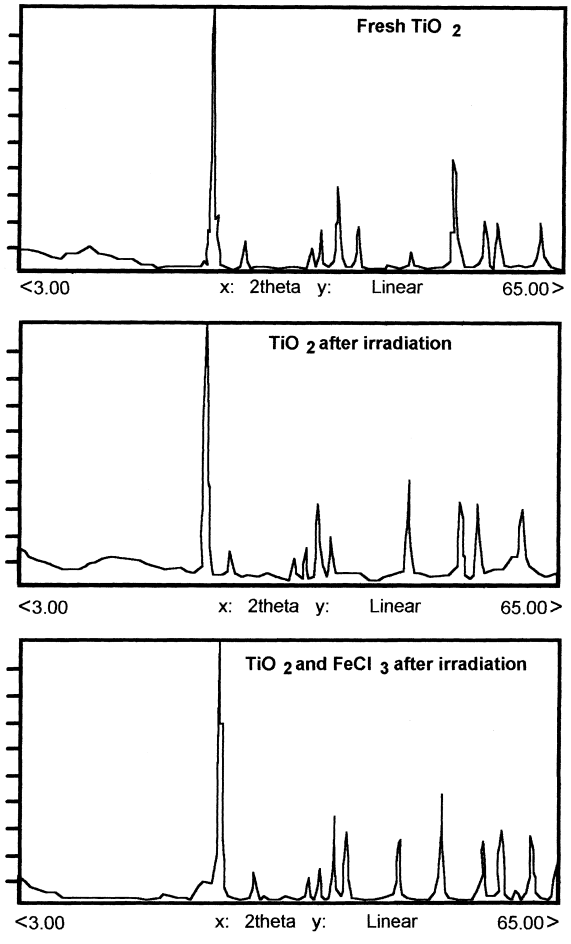

Fig. 15. X-ray diffractometry for: (a) fresh TiO_2; (b) TiO_2 after irradiation; (c) TiO_2 and $FeCl_3$ after irradiation.

This effect was also observed for the photo-oxidation of DBS.

7.4. Deactivation of catalyst

Several runs were made in order to study the deactivation of TiO_2. From these experiments, a decrease in the activity of TiO_2 after first irradiation was observed, and after that the activity remained constant for long time. Data of Ω vs. time are plotted in Fig. 14.

Attempts were made to regenerate the catalyst by flowing through it steam at 4–6 bar for 2–3 h, but the catalyst could not be regenerated (Fig. 14).

However, when the catalyst was used with a $FeCl_3$ solution, the activity of TiO_2 remained constant during all experiments and the same as that for the fresh catalyst.

In order to have more information about that, a study of TiO_2 catalyst was made by X-ray diffraction, differential thermal analysis (DTA) and thermo gravimetrical analysis (TG) (Fig. 15 abd 16). The TiO_2 used was Carlo-Erba with 75% de anatase (active form) and 25% of rutile, when it was irradiated, the X-ray diffraction showed that the composition was 70% anatase and 30% rutile, therefore the activity decreased because part of the active form (anatase) is changed to rutile. When $FeCl_3$ solution was added, no change in the structural composition was observed (Fig. 15).

Rives and coworkers [12] showed that when TiO_2 crystals are doped with Fe^{3+} the activity of catalyst decreases, which is logical because part of Ti^{4+} is replaced by Fe^{3+}, but in our case with a solution of $FeCl_3$, the activity of TiO_2 remained constant.

In order to check the possibility of the formation of some intermediate compound, TG and DTA were performed (Fig. 16). From these data, it can be deduced that no intermediates were formed because

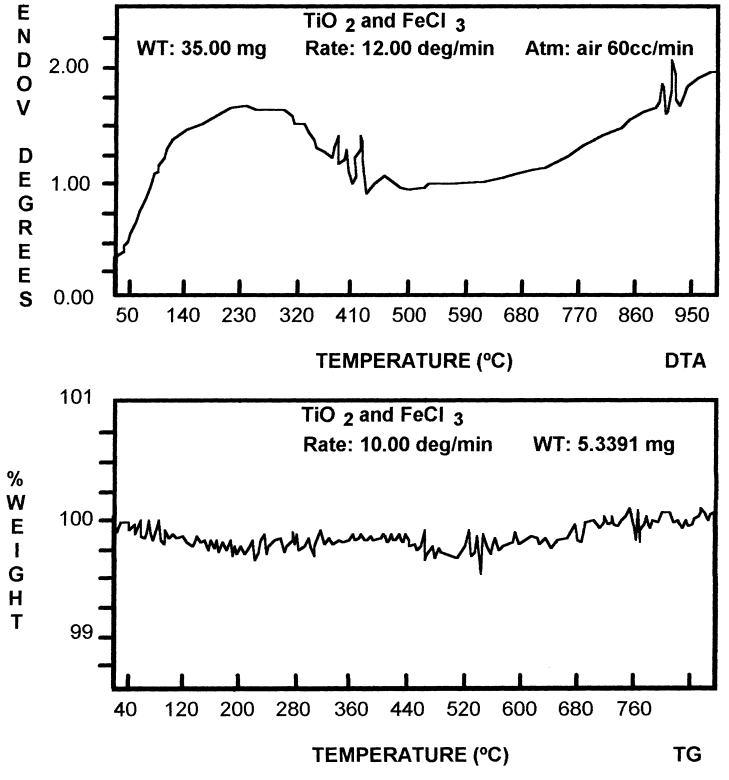

Fig. 16. (a) DTA; (b) TG for used TiO_2 and $FeCl_3$ after irradiation.

no weight lost was recorded and the only peaks were for FeO_3 at 383°C and $Fe(OH)_3$ at 948°C.

8. Conclusion

Kinetics of photodecomposition of aqueous solutions of DBS, azynphos-methyl and dimethoate has been studied in a differential tubular reactor and a parallel-plate reactor by using solar light with and without $FeCl_3$ and TiO_2 as photosensitizer and catalyst, respectively.

With solar light, DBS does not decompose, but with solar light and using $FeCl_3$ as photosensitizer, the DBS is decomposed. When TiO_2 is used instead of $FeCl_3$, DBS is decomposed with a rate almost two times greater than that for $FeCl_3$; and when TiO_2 and $FeCl_3$ are used together, the decomposition rate is almost three times greater than that for $FeCl_3$ only.

Solar light decomposes very slowly the azynphos-methyl, but when solar light is used with TiO_2 and $FeCl_3$ the rate increases 10^5 times, and in case that $FeCl_3$ and TiO_2 are used together, then the decomposition rate is increased 10 times compared to decomposition with $FeCl_3$ or TiO_2.

In case of dimethoate, we observe a similar performance, when $FeCl_3$ or TiO_2 is used, the rate increased in the same way as that for azynphos-methyl: 10^5 times, and 10 times more when $FeCl_3$ is used together with TiO_2.

Matsuura and Smith [4] suggested an initial rapid conversion of DBS into a primary intermediate and after a slower photo-oxidation which leads to small oxygenated organic compound, with evidence of destruction of aromatic ring structure.

No evidences of the ring structures, as benzoquinone, etc. were found for the oxidation of azynphos-methyl by using our analytical techniques.

From all this work, it can be concluded that solar light can be used together with small amount of $FeCl_3$ and TiO_2 for a tertiary treatment, to eliminate pollutant as detergents or pesticides in a short time, by using a tank, with TiO_2 fixed as a paint in the bottom, and using reflectors (specular aluminum) for the sun light, following a green filter. We assume that this can be very cheap and can be used in farms or villages in the country side for water remediation.

9. Nomenclature

C_i	concentrations, gmol/cm^3
C_λ	albedo, defined by Eq. (23)
D	thickness of film of water
F_λ	energy output of the lamp at λ, einst/s
F_t	total polychromatic energy output of lamp, einst/s
h	Planck's constant
I_a	absorbed light intensity, einst/cm^3 s
$I_{a,\lambda}$	absorbed light intensity at wavelength λ, einst/cm^2 s
$I_{Fe^{3+}}$	absorbed light intensity by Fe^{3+}, einst/cm^2 s
$I_{\lambda,\omega}$	light intensity by absorption at wavelength λ in the LSSE model, einst/cm^2 s
$I_{\lambda,\omega}$	light intensity by scattering at wavelength λ in the LSSE model, einst/cm^2 s
I_0	intensity of radiation reaching the wall of reactor, einst/cm^2 s
$I_{0,\lambda}$	intensity of radiation reaching the wall of reactor at wavelength λ, einst/cm^2 s
k_i, K, K^*	kinetic constants, c.g.s. units
m_λ	optical thickness, defined by Eq. (22)
P_λ	coefficient of probability of scattering of photons
$P(\omega',\omega)$	coefficient of probability of dispersion between ω and ω'
Q	volumetric flow-rate, defined by Eq. (26), cm^3/s
R	outer radius of the reactor annulus, cm
T_λ	fraction of radiation at wavelength λ transmitted through filter solution
V_S	irradiated volume of reactor, cm^3
V_R	total volume of liquid in batch-recycle reactor, cm^3

Greek letters

η	axial coordinate, defined by Eq. (18)
μ	attenuation coefficient, defined by Eq. (22), cm^{-1}
ν	frequency, s^{-1}
ρ	spherical coordinate, cm
σ_λ	dispersion coefficient at wavelength, defined by Eq. (22), cm^{-1}
Φ_λ	quantum yield at wavelength, g mol/einst

Ω solid angle, sr
Ω_i rate or decomposition, gmol/cm^3 s

Acknowledgements

We will like to express our thanks to General Química S.A. for providing the samples of azynphos-methyl and dimethoate.

References

[1] P.L. Yue, F. Khan, L. Rizzuti, Chem. Eng. Sci. 38 (1983) 1893–1900.
[2] D. Ollis, Lett. Catal. 66 (1980) 383–390.
[3] M.A. Torres, M.S. Thesis, Univ. Cádiz, Spain, 1986.
[4] T. Matsuura, J.M. Smith, Ind. Eng. Chem. Fundam. 9(2) (1970) 252–260.
[5] T. Matsuura, J.M. Smith, Ind. Eng. Chem. Fundam. 10(2) (1971) 316–318.
[6] A. Chukundobe, R.B. March, M. Othman, T.R. Fukuto, J. Agric. Food Chem. 37 (1989) 539–545.
[7] F.J. Beltrán, G. Ovejero, J.F. García-Arraya, J. Rivas, Ind. Eng. Chem. Res. 34 (1995) 1607–1615.
[8] M.A. Galán, J.M. Smith, Chem. Eng. Sci. 31 (1976) 1047–1056.
[9] S.M. Jacob, J.S. Dranoff, AIChE J. 16 (1970) 359–363.
[10] O.M. Alfano, R.L. Romero, A. Cassano, Chem. Eng. Sci. 41 (1986) 1137–1153.
[11] G. Spadoni, F. Bandani, F. Santarelli, Chem. Eng. Sci. 33 (1978) 517–524.
[12] L. Palmisano, M. Schiavello, A. Sclafani, C. Martín, I. Martín, V. Rives, Catal. Lett. 24 (1994) 303–315.